09,08

Photoluminescence of ytterbium doped zirconia

© S.N. Shkerin[1], E.S. Ulyanova[2], E.G. Vovkotrub[1]

[1] Institute of High-Temperature Electrochemistry, Ural Branch, Russian Academy of Sciences, Yekaterinburg, Russia
[2] Institute of Solid State Chemistry, Russian Academy of Sciences, Ural Branch, Yekaterinburg, Russia

E-mail: shkerin@mail.ru

Received December 6, 2021
Revised December 6, 2021
Accepted December 15, 2021

Raman spectra were studied for the cubic ytterbium doped zirconia with 10, 20 and 25% of dopant. This part of investigation deals with region of large wave numbers. Two different excitation sources with wavelength 785 and 532 nm are used. For first time Stokes lines that are independent of the excitation wavelength were observed together with conventional luminescence of ytterbium cation.

Keywords: $Zr(Yb)O_2$, Raman spectroscopy, photoluminescence, the crystal defects association.

DOI: 10.21883/PSS.2022.04.53502.252

1. Introduction

Doped zirconium dioxide is widely used as a solid oxygen-conducting electrolyte in high-temperature electrochemical devices [1–10]. Prediction of the properties of such electrolytes requires understanding of their defect structure and, especially, the interaction of point defects with each other. Such interaction gives rise to a particular behavior of the material near-surface layer [11–13], grain boundaries [14,15], conduction [16–18], including its stability over time [19–21], thermal conductivity anomalies at low temperatures [22,23]. There are not many methods for studying the short-range order. The most easily available of them are oscillation spectroscopy methods. However, Raman scattering spectra, which usually yield one band with T_{2g} symmetry for materials with a FCC-structure of the fluorite type [24], show a considerably more complex situation for zirconium dioxide-based materials. An example of such complex spectra for single-crystal samples is given in [25]. An analysis of light scattering mechanisms [26] shows that Stokes bands can be separated from other effects by means of monochromatic source with a different wavelength, because only linear Stokes effects are independent from wavelength of superimposed perturbation. This is demonstrated in [27] using four different lasers for analysis of cerium dioxide and several oxides of rare earth metals. In the first part of this paper, two different monochromatic light sources with the wavelengths of 532 and 785 nm were used to distinguish Stokes lines, which allowed for studying the short-range order of zirconium dioxide-based materials using an analysis of reliably Stokes lines [28].

The use of cations with f-electrons (rare earth metals, REM) as a dopant opens up new opportunities. Transitions between f-levels of localized REM-metals have been studied well. Injection of such cations into a medium leads to energy level splitting under the action of the field which surrounds the cation. A contribution to this splitting is also made by coordination surrounding with anions which, in principle, makes it possible to determine the cation coordination number. However, these effects are weak and require a well-considered selection of a REM-cation. The ytterbium cation favorably differs by a small number of active lines [29], which increases noise immunity of such experiments. Influence of environment symmetry on band splitting $F_{7/2} \rightarrow F_{5/2}$, observed at a wavelength of approximately 980 nm, has been already considered for the ytterbium cation, though in a fluoride matrix of fluorite CaF_2 [30]. There are few papers on the study of ytterbium luminescence in oxide matrices [31–34], and we have not found any paper on photoluminescence for zirconium dioxide with a FCC-structure of the fluorite type. The present paper studies the splitting of the ytterbium cation luminescence band in an oxide matrix with the $Zr(Yb)O_2$ fluorite structure. Luminescence was studied using Raman scattering instruments, as a manifestation of effects in the region of large wave numbers.

2. Experimental part

2.1. Sample preparation

Samples were made by inverse coprecipitation of hydroxides in aqueous ammonia. The initial materials were: zirconium oxychloride $ZrOCl_2 \cdot 8H_2O$ (99%), ytterbium oxide (99.995%), nitric acid (99%) and aqueous ammonia. Aqueous ammonia was prepared by dissolving gaseous ammonia in distilled water; ytterbium oxide was dissolved in nitric acid. The hydroxide sediment was washed with distilled water and ethanol, dried at 120°C, rubbed up, baked at 750°C, again rubbed up, pressed into samples with the diameter of 15 mm at 200 MPa and sintered in a vacuum

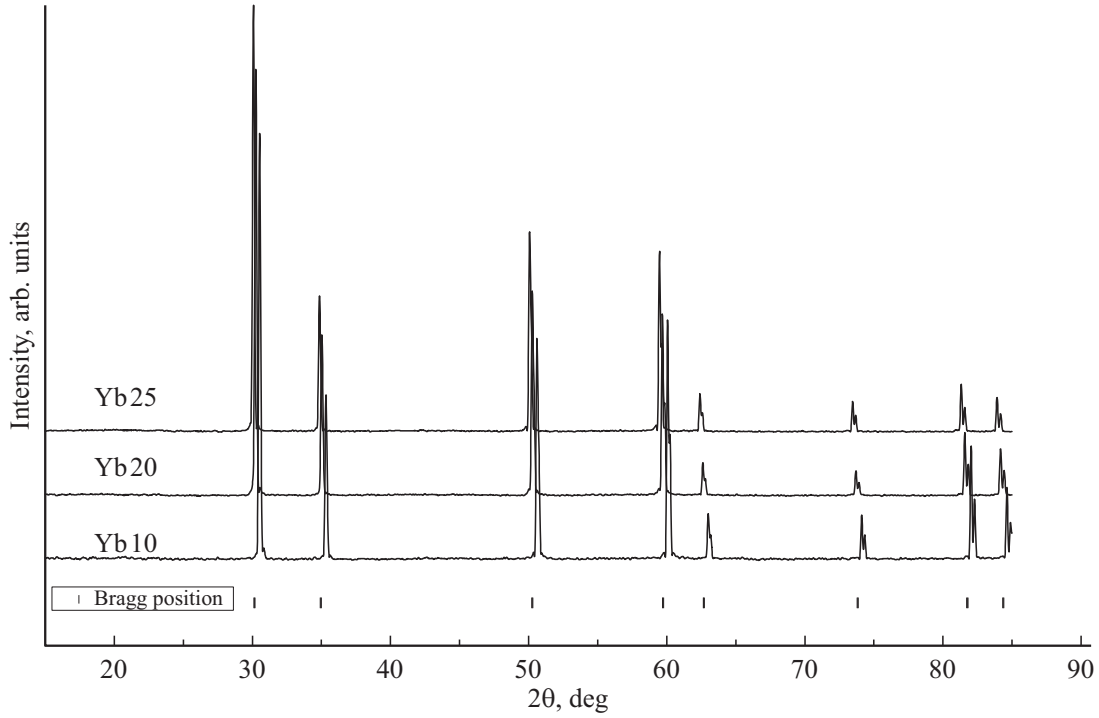

Figure 1. Diffraction patterns for the studied samples. The vertical dashes show the positions of the lines according to the description in the $Fm\bar{3}m$ symmetry group.

Table 1. Cubic lattice parameters of the $(1-x)ZrO_2 + xYb_2O_3$ samples and the $0.9\,ZrO_2 + 0.1\,Y_2O_3$ reference sample

Sample	Yb 10	Yb 20	Yb 25	YSZ 10
Composition	$0.1\,Yb_2O_3 + 0.9\,ZrO_2$	$0.2\,Yb_2O_3 + 0.8\,ZrO_2$	$0.25\,Yb_2O_3 + 0.75\,ZrO_2$	$0.1\,Y_2O_3 + 0.9\,ZrO_2$
a, Å	5.110(3)	5.136(2)	5.1514(7)	5.152(1)

furnace at 1900°C (1 h). After the vacuum furnace, the samples were annealed in the air at 1650°C (5 h).

Samples of commercial zirconium dioxide ceramics, doped with ten percent of yttrium oxide, were used to distinguish the ytterbium-induced effects.

2.2. X-ray study

Sample qualification and phase composition check were performed by powder X-ray diffraction (XRD) using a Rigaku D/MAX-2200VL/PC diffractometer (RIGAKU) in Cu-K_α radiation ($\lambda = 1.5418$ Å) with the interval of $\Delta 2\theta \approx 0.02°$ with the angular scanning rate of 1.2°/min at room temperature in air atmosphere. Phase composition analysis and calculation of crystallographic parameters were performed using the MDI Jade 6.5 software package (Materials Data Incorporated. 2551 Second Street Livermore, California 94550, 2011) and the PDF-2 ICDD database (Powder Diffraction File PDF2 ICDD Release 2004).

2.3. Studies by Raman scattering method

Studies by Raman scattering method were performed using two different instruments:

– green radiation ($\lambda = 532$ nm) using a Renishaw U 1000 microscope-spectrometer. Power of the Nd:YAG laser was 50 mW;

– red radiation ($\lambda = 785$ nm) using InVia Reflex with a Leica DM2700 microscope. Power of the Renishaw diode laser with an integrated plasma filter was 300 mW.

Spectrum accumulation time is from 10 to 30 s, number of passes is from 5 to 16.

3. Results and discussion

The diffraction experiment results are shown in Fig. 1. The sample structure can be described as cubic, with symmetry group $Fm\bar{3}m$, ($Zr_{0.8}Yb_{0.2}O_{1.9}$ PDF №78–1309). The lattice parameters, together with name and chemical composition, are given in Table 1.

Table 2. Bands, frequency ν (cm^{-1}) and half-width D (cm^{-1}) observed on the samples in the region of large wave numbers under excitation by different light sources

	Yb 10				Yb 20				Yb 25				YSZ 10	Luminescence	
	Red, 785 nm		Green, 532 nm		Red, 785 nm		Green, 532 nm		Red, 785 nm		Green, 532 nm		532 nm	λ, nm	E, eV
	ν	D	ν	D	ν	D	ν	D	ν	D	ν	D			
							1683.0	*121.4*							
							1704.7	*42.4*							
LG1			1711.7	18.0			1712.6	18.4			1710.6	22.8	1711.9	585.3	2.118
LG2			1762.3	51.1			1759.5	75.0			1752.3	93.1	1753.0	586.9	2.112
A1	1768.9	236.4	1770.3	12.8										–	–
			1773.0	105.8											
LG3			1822.4	53.7			1824.8	54.3			1830.1	47.0	–	589.2	2.104
LG4			1871.7	60.0			1871.4	65.9			1870.3	63.6	1863.8	590.8	2.098
LG5			1957.6	111.6			1954.3	121.3			1950.0	120.9	–	593.7	2.088
LG6			2073.4	528.4			2067.3	124.8			2036.1	184.6	–	597.5	2.075
LR1	2134.9	362.6			2137.1	296.1			2149.8	253.4				942.9	1.315
LG7			2225.1	58.5			2238.9	54.4			2227.2	60.8	–	603.6	2.054
X1	2263.7	90.9	2295.7	97.4	2288.1	92.0	2309.7	102.0	2292.0	80.8	2267.7	92.3	2281.3	–	–
							2327.7	*5.4*							
X2	2367.9	49.7	2387.0	136.0	2387.7	50.8	2423.1	93.4	2390.8	43.1	2368.3	31.2		–	–
(?)							2424.4	537.3			2406.3	158.9			
					2462.0	202.8									
LR2	2428.6	24.0			2436.9	43.2									
MAX	2447.8	107.1			2444.7	75.9			2441.9	57.8				971.7	1.276
A2	2562.7	124.3	2557.9	342.7					*2454.7*	*193.3*				–	–
LR3	2668.1	209.6			2693.0	201.1			2690.3	228.4				993.1	1.248
							2719.7	*320.8*							
LG8			2922.7	124.1			2917.9	192.2			2947.5	161.1		630.2	1.967
LG9			3025.3	78.6			3007.4	146.3			3000.8	85.3	2995.7	633.4	1.957

The results of sample study by the Raman scattering method are shown in Fig. 2 and 3. In Fig. 2, the results with the use of a green ($\lambda = 532$ nm) laser demonstrate, in addition to the well-known, e.g. [25], lines in the region of up to 800 cm^{-1}, a set of bands in the region of wave numbers exceeding one thousand of reciprocal centimeters. Reflections in this frequency region are usually identified as a manifestation of luminescence. Fig. 3 shows the results of study using a red ($\lambda = 785$ nm) laser. A multiplet of a very high intensity is observed in the long-wavelength part of the spectrum at wave numbers 2300–2600; the multiplet is due to luminescence caused by a $F^{7/2} \rightarrow F^{5/2}$ transition of the ytterbium cation [29–34].

The „Peak separation 2“ software package was used to describe the observed spectra by a combination of Gaussian curve lines. An example of such description is given in Fig. 4. The combination of results obtained using both red ($\lambda = 785$ nm) and green ($\lambda = 532$ nm) lasers is given in Table 2. The series of bands designated in Table 2 as LR1–LR3 are observed only in the red laser spectra (Fig. 5), while the series of bands designated as LG1–LG9 is observed only in the green laser spectra.

At the same time it should be noted that there are lines present simultaneously in the red and green laser spectra (X1 in Fig. 5). This indicates the Stokes nature of these lines. Only high-order Stokes lines are observed in this region of wave numbers [35]. As far as we know, this effect for doped zirconium dioxide is reported for the first time.

The Stokes line X1 (Fig. 6) has a high intensity. Of course, it is weaker than the band caused by a $F^{7/2} \rightarrow F^{5/2}$ transition of the ytterbium cation under excitation by a red laser, but it is stronger than all the luminescence bands observed in the green laser (Fig. 6).

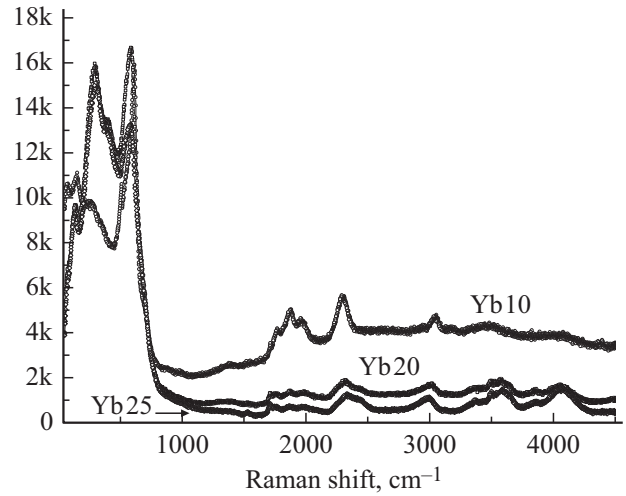

Figure 2. Raman scattering spectra. $\lambda = 532$ nm

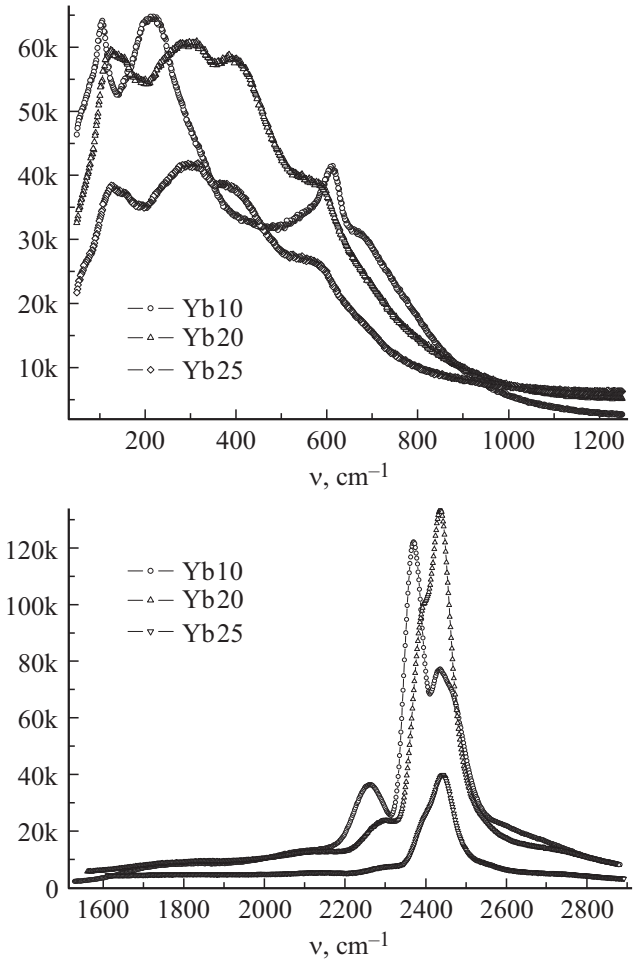

Figure 3. Raman scattering spectra using the red ($\lambda = 785$ nm) laser for samples. The region of small wave numbers is in the top, that of large ones is in the bottom.

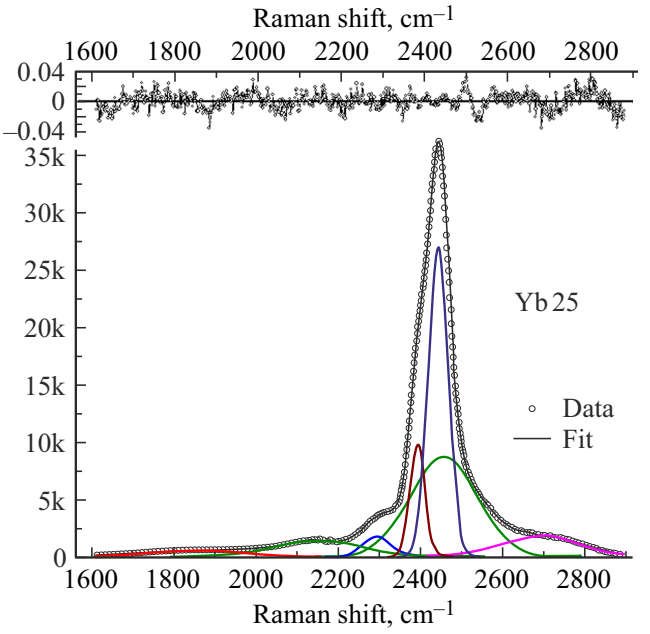

Figure 4. Example of description of Yb25 sample spectrum, a combination of Gaussian bands. The figure top shows the relative error.

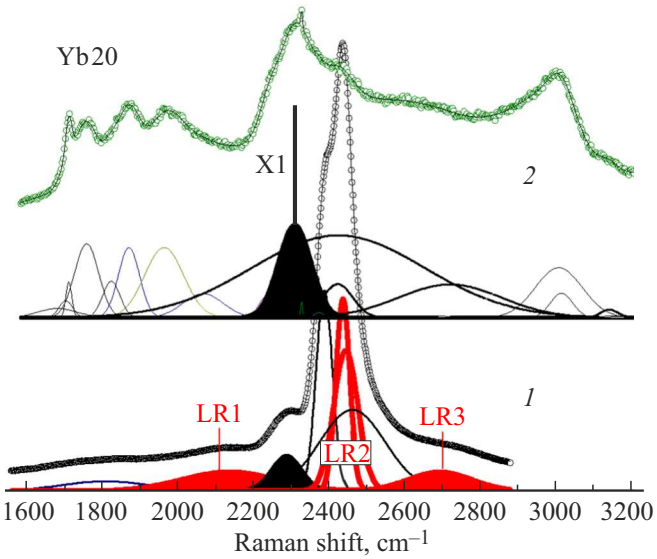

Figure 5. Comparison of red (*1*) and green (*2*) radiation spectra for the Yb 20 sample. Band X1 is present in both spectra. Bands LR1–LR3 are present only in the spectra with the use of the red laser.

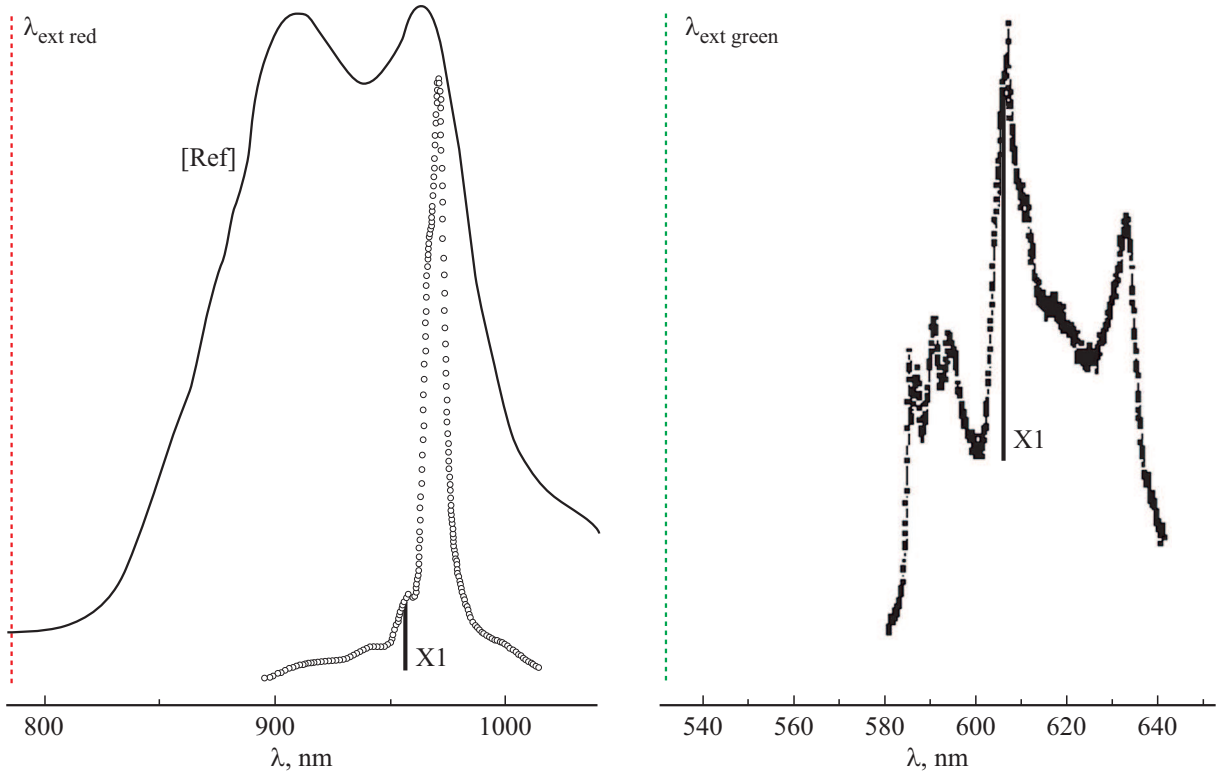

Figure 6. Luminescence spectra obtained in red (left) and green (right) radiation. The vertical dashed lines show the excitation radiation wavelength. The heavy line X1 shows the Stokes band. For comparison we give the spectrum (Ref) for X-ray stimulated luminescence of the composition similar to Yb20 [34].

Apparently, band X1 is not the only Stokes line for these materials. Fig. 7 compares the spectra obtained using both the red laser ($\lambda = 785$ nm) and the green laser ($\lambda = 532$ nm). In addition to the intensive band X1, we also observe two bands A1 and A2, which have a considerably lower intensity, but they seem to be of a Stokes pattern as well, since they are present in the spectra obtained using both the red and green lasers. As distinct from band X1, present in the spectra of all compounds, lines A1 and A2 are present only for compound Yb10.

A band caused by a $F^{7/2} \rightarrow F^{5/2}$ transition of the ytterbium cation is observed when using the red laser for all the ytterbium-containing samples (Table 2) and is absent for the yttrium-doped sample. It is the source of the strongest luminescence for the given samples and is described in literature. A new result is the splitting of this band into a well-separated triplet LG1–LG3 (Fig. 5), from which the band LG2 itself is, apparently, is a multiplet. A similar splitting has been studied earlier for the ytterbium cation in the CaF_2 matrix, which is isostructural to the materials under our study [30]. An analysis of such splitting provides prospects of the use of the ytterbium cation environment.

Luminescence under the green laser action has a low intensity. Hypothetically, a source of such luminescence can also be the ytterbium cation, for which weak-intensity effects have been reported earlier [29,36–39]. An alternative reason can be luminescence due to radiation transitions between the conduction band and trap states of doped zirconium dioxide, such as oxygen vacancy V_0, bonded complexes of an oxygen vacancy and a doping cation [40–42].

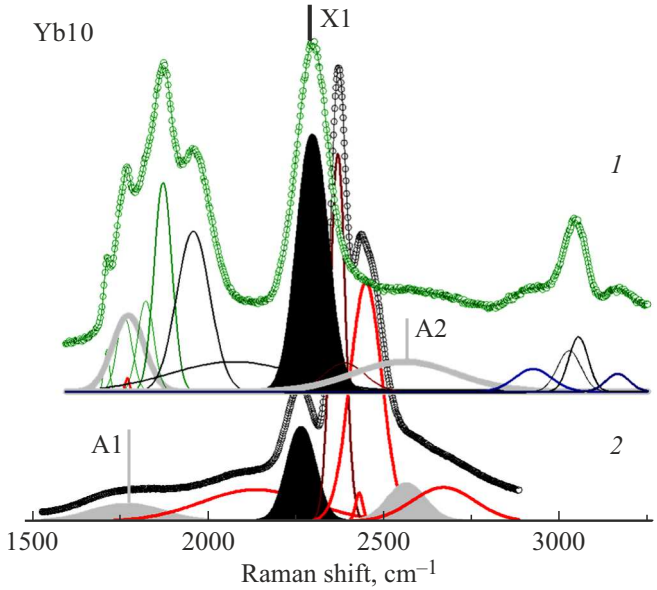

Figure 7. Comparison of red (*1*) and green (*2*) radiation spectra for the Yb 10 sample. Band X1 is present in both spectra for all compounds, while bands A1 and A2 are present only for Yb 10.

Such effects are not related to the ytterbium cation and require further study.

4. Conclusion

We studied the Raman scattering spectra for the zirconium dioxide samples doped with 10, 20 and 25% of ytterbium oxide in the region of large wave numbers. We used two different monochromatic sources with a different wavelength (532 and 785 nm), which makes it possible to distinguish Stokes lines. A band caused by a $F^{7/2} \rightarrow F^{5/2}$ transition of the ytterbium cation is observed when using the red laser. Splitting is described for the first time for an oxide matrix with the fluorite structure (Fig. 5).

We show the presence of Stokes lines, occurrence of which does not depend on source wavelength. It has been done for the first time in this region of wave numbers for oxide materials with the fluorite structure. The lines were interpreted as high-order Stokes lines.

Luminescence under the green laser action, the existence of which was described earlier, is confirmed.

Acknowledgments

The study was performed using the equipment at the Shared Access Center of the Institute of High Temperature Electrochemistry of the Ural Branch of RAS with participation of A. Akhmadeyev. The authors would like to thank V.P. Gorelov for the samples.

Funding

The study was performed within the framework of the state funding program (topic registration number AAAA-A19-119020190044-1) at the Institute of High Temperature Electrochemistry of the Ural Branch of RAS.

Conflict of interest

The authors declare that they have no conflict of interest.

References

[1] V.N. Chebotin, M.V. Perfilyev. Elektrokhimiya tverdykh elektrolitov. Khimiya, M. (1978). 312 p. (in Russian) [Republished by Washington: Technical Information Center, U.S. Department of Energ (1984).].
[2] M.V. Perfilyev, A.K. Demin, B.L. Kuzin, A.S. Lipilin. Vysokotemperaturny elektroliz gazov. Nauka, M. (1988). 232 p. (in Russian).
[3] V.N. Chebotin. Khimicheskaya diffuziya v tverdykh telakh. Nauka, M. (1989). 208 p. (in Russian).
[4] M. Balkanski, T. Takahashi, H. Tuller. Solid State Ionics. Elsevier, Amsterdam (1992). 345 p.
[5] A.K. Ivanov-Shits, I.V. Murin. Ionika tverdogo tela. SPbSU, SPb (2000). Vol. 1. 616 p. (in Russian).
[6] S.C. Singha, K. Kendall. High temperature solid oxide fuel cells: fundamentals, design and applications. Elsevier (2003). 429 p.
[7] J. Maier. Physical chemistry of ionic materials: ions and electrons in solids. John Wiley & Sons (2004). 539 p.
[8] A.K. Ivanov-Shits, I.V. Murin. Ionika tverdogo tela. SPbSU, SPb (2010). Vol. 2. 1000 p. (in Russian).
[9] F. Ramadhani, M.A. Hussain, H. Mokhlis, S. Hajimolana. Renew. Sust. Energ. Rev. **76**, 460 (2017).
[10] T. Liu,, X. Zhang, X. Wang, J. Yu, L. Li. Ionics **22**, 2249 (2016).
[11] S.N. Shkerin. Izv. RAN. Ser. fiz. **66**, 890 (2002) (in Russian).
[12] S. Shkerin. Fuel Cell Technologies: State and Perspectives, NATO Science Ser. Mathematics, Physics and Chemistry. Springer **202**, 301 (2005).
[13] V. Ivanov, S. Shkerin, A. Rempel, V. Khrustov, A. Lipilin, A. Nikonov. J. Nanosci. Nanotechnol. **10**, *11*, 7411 (2010).
[14] V.V. Ivanov, S.N. Shkerin, A.A. Rempel, V.R. Khrustov, A.S. Lipilin, A.V. Nikonov. Dokl. RAN **433**, *2*, 206 (2010) (in Russian).
[15] A.N. Vlasov. Elektrokhimiya **25**, *5*, 699 (1989) (in Russian).
[16] A.N. Vlasov. Elektrokhimiya **25**, *10*, 1313 (1989) (in Russian).
[17] A.N. Vlasov. I.G. Shulik. Elektrokhimiya **26**, *7*, 909 (1990) (in Russian).
[18] A.N. Vlasov. Elektrokhimiya **19**, *2*, 1624 (1983) (in Russian).
[19] A.N. Vlasov, M.V. Inozemtsev. Elektrokhimiya **21**, *6*, 764 (1985) (in Russian).
[20] A. Vlasov, M.V. Perfiliev. Solid State Ionics **25**, 245 (1987).
[21] A.N. Vlasov. Elektrokhimiya **27**, *11*, 1479 (1991) (in Russian).
[22] M.A. Borik, A.V. Kulebyakin, I.E. Kuritsyna, E.E. Lomonova, V.A. Myzina, P.A. Popov, F.O. Milovich, N.Yu. Tabachkova. FTT **61**, *12*, 2390 (2019) (in Russian).
[23] D.A. Agarkov, M.A. Borik, G.M. Korableva, A.V. Kulebyakin, I.E. Kuritsyna, E.E. Lomonova, F.O. Milovich, V.A. Myzina, P.A. Popov, P.A. Ryabochkina. FTT **62**, *12*, 2093 (2020) (in Russian).
[24] V.G. Keramidas, W.B. White. J. Chem. Phys. **59**, *3*, 1561 (1973).
[25] E.E. Lomonova, D.A. Agarkov, M.A. Borik, G.M. Yeliseeva, A.V. Kulebyakin, I.E. Kuritsyna, F.O. Milovich, V.A. Myzina, V.V. Osiko, A.S. Chislov, N.Yu. Tabachkova. Elektrokhimiya **56**, *2*, 127 (2020) (In Russian).
[26] D.A. Long. The Raman effect: A unified treatment of the theory of raman scattering by molecules. John Wiley & Sons Ltd (2002). 610 p.
[27] J. Cui, G. Hope. J. Spectrosc. (Hindawi) **2015**, Article ID 940172 (2015). http://dx.doi.org/10.1155/2015/940172
[28] S.N. Shkerin, E.S. Yulyanova, E.G. Vovkotrub. Neorgan. materialy **57**, *11*, 1213 (2021) (in Russian).
[29] Yu.K. Voronko, B.I. Denker, V.V. Osiko. FTT **13**, *8*, 2193 (1971) (in Russian).
[30] T. Kallel, M.A. Hassairi, M. Dammak, A. Lyberis, P. Gredin, M. Mortier. J. Alloys Compd. **584**, 261 (2014).
[31] W. Tang, Y. Wang, C.-L. Jia. FTT **63**, *1*, 110 (2021) (in Russian).
[32] Y. Yu, Y. Huang, L. Zhang, Z. Lin, G. Wang. PLoS ONE **8**, *1*, e54450 (2013). doi: 10.1371/journal.pone.0054450
[33] L. Zhenzhang, Z. Shaoan, X. Qinfang, D. He, L. Yang, L. Xiaohui, W. Chuanlong, J. Jin, H. Yihua. J. Alloys Compd. **766**, 663 (2018).

[34] R. Khabibrakhmanov, A. Shurukhina, A. Rudakova, D. Barinov, V. Ryabchuk, A. Emeline, G. Kataeva, N. Serpone. Chem. Phys. Lett. **742**, 137136 (2020).
[35] S. Prawer, R. Nemanich. Phil. Trans. R. Soc. A. **362**, 2537 (2004).
[36] G. Broden, S.B.Y. Hagstrom T.L. Loucks. Phys. Rev. Lett. **21**, 1524 (1968).
[37] J.G. Endriz, W.E. Spicer. Phys. Rev. B **2**, 1466 (1970).
[38] P.O. Heden, H. Lofgren, S.G.Y. Hagstrom. Phys. Status Solidi B **49**, 721 (1972).
[39] Y. Baer, G. Busch. J. Electron Spectrosc. Rel. Phenom. **5**, 627 (1974).
[40] N.G. Petrik, D.P. Taylor, T.M. Orlando. J. Appl. Phys. **85**, 6770 (1999).
[41] Z. Wanga, Z.Q. Chena, J. Zhua, S.J. Wanga, X. Guo. Rad. Phys. Chem. **58**, 697 (2000).
[42] J. Costantini, F. Beuneu, M. Fasoli, A. Galli, A. Vedda, M. Martini. J. Phys.: Condens. Matter **23**, 11590 (2011).